

Active reduction of vibroacoustic transmission using elasto-poroelastic sandwich panels and piezoelectric materials

T.G. Zieliński¹, M.-A. Galland¹, M.N. Ichchou²

¹ LMFA, Centre Acoustique UMR CNRS 5509
Ecole Centrale de Lyon, 36 av. Guy de Collongue, 69134 Ecully Cedex, France

² LTDS, Equipe Dynamique des Systèmes et des Structures UMR CNRS 5511
Ecole Centrale de Lyon, 36 av. Guy de Collongue, 69134 Ecully Cedex, France

The paper addresses the issue of an active sandwich panel made of elastic faceplates and a poroelastic core. The panel is supposed to be active thanks to piezoelectric patches glued to the one of elastic layers. This piezoelectric actuator is used to excite the panel vibrations in the low frequency range with the aim to reduce the transmitted wave. A complete description of the sandwich behaviour is obtained using a finite element model implemented in FEMLAB[®] environment. The poroelastic material is modeled using a recent formulation (by Atalla et al.) valid for harmonic oscillations, but the classical Biot formulation is also implemented. Coupling occurring between poroelastic material and plates, and between elastic plate and piezoelectric patches is fully considered. The achieved numerical model allows prediction of transmission coefficient for plane waves under normal incidence. Hence, some numerical experiments can be offered for multiple assembly configurations whose ultimate goal is to determine the best assembly and the best control strategy for reducing the transmission over a wide frequency range.

1 Introduction

Porous materials has been widely used as very effective and in fact the most vital components of noise mufflers. It is a well-known fact that vibroacoustic transmission of high frequency range can be *passively* reduced by mufflers made of appropriately chosen layer(s) of porous materials. However, it has been also recognized that when the lower frequencies are dominant, an *active* approach to the noise reduction is necessary. These facts shall be once again illustrated in the present paper where we propose and analyse an active sandwich panel as a possible solution to the problem of reduction of broad spectrum noise. The core of sandwich panel is made of porous material and is responsible (working together with the elastic faceplates of bigger mass) for the passive noise reduction; the active reduction can be achieved thanks to a piezoelectric actuator. The whole panel was modeled using FEMLAB[®] environment. It is important to notice here that for many porous materials, in lower frequencies, a more complicated but at the same time, more realistic, poroelastic modeling usually needs to be used, and it is indispensable in vibroacoustic applications. Since the modeling of poroelasticity in FEMLAB[®] is by no means trivial, a short description of poroelastic models as well as their convincing validation constitute the first part of this paper. In the second part, the results of FE analysis of sandwich panel are given.

2 Poroelasticity: modeling using FEMLAB[®]

2.1 Two formulations of isotropic poroelasticity

The Biot's displacement formulation. In 1956 Biot [1, 2] presented the theory of poroelasticity where the behaviour of the two-phase porous medium is completely described by the displacements of solid and fluid phases. Therefore, this classical formulation can be called by the name of the *displacement formulation* ($u-v$). Biot derived the *equations of equilibrium* where partial stress tensors associated with the skeleton particle and the macroscopic fluid particle are (independently) linked with the solid and fluid macroscopic displacements. Therefore, in these poroelasticity equations of motion there are some important terms responsible for the coupling between the solid and fluid phase: these terms depend on the so-called mass coupling coefficient and viscous damping coefficient. Biot provided also the *constitutive relations* where the partial stress tensors are linearly related to the partial strain tensors prevailing in the skeleton and the interstitial fluid. In these equations there are only 4 material constants: the shear modulus of porous material (which, consequently, is the shear modulus of frame) and three dilatational Lamé-like coefficients (they are functions of bulk moduli of: the material of frame, frame in vacuum, and fluid). One of these coefficients refers to the isotropic fluid phase, another one – together with the shear modulus – to the isotropic solid phase, and finally (only) one is responsible for the constitutive coupling between both phases. The *kinematic equations* for poroelastic medium are (non-coupled) classical kinematic relations of linear elasticity and fluid mechanics. Combining all these equations

together results in the set of partial differential equations which forms the *displacement equations of (isotropic, linear) poroelasticity*. Below, we present these equations for the case of harmonic motion (with the angular frequency ω) of a poroelastic medium with constant material properties:

$$\begin{aligned} (\tilde{\lambda}^s + \mu^s)u_{j|j i} + \mu^s u_{i|j j} + \omega^2 \tilde{\varrho}_{11} u_i + \overbrace{\tilde{\lambda}^{\text{fs}} v_{j|j i} + \omega^2 \tilde{\varrho}_{12} v_i}^{\text{coupling terms}} &= 0, \\ \underbrace{\tilde{\lambda}^{\text{fs}} u_{j|j i} + \omega^2 \tilde{\varrho}_{12} u_i}_{\text{coupling terms}} + \tilde{\lambda}^f v_{j|j i} + \omega^2 \tilde{\varrho}_{22} v_i &= 0. \end{aligned} \quad (1)$$

Here μ^s , $\tilde{\lambda}^s$, $\tilde{\lambda}^f$, $\tilde{\lambda}^{\text{fs}}$ are the four material constants of isotropic poroelasticity, whereas $\tilde{\varrho}_{11}$, $\tilde{\varrho}_{22}$, $\tilde{\varrho}_{12}$ are the frequency-dependent effective densities. The coefficients $\tilde{\lambda}^{\text{fs}}$ and $\tilde{\varrho}_{12}$ are responsible for the mentioned constitutive and equilibrium coupling, respectively. Since the unknowns are the displacements of solid, u_i , and fluid phase, v_i , then we shall have 6 DOFs in every point of 3D poroelastic model.

The mixed displacement-pressure formulation. In 1998 Atalla *et al.* [3, 4] proposed the so-called *displacement-pressure formulation (u-p)* which, in fact, is a variation of the Biot's model – however, valid only for harmonic oscillations. In this case, the fluid displacements, v_i , can be excluded completely from the Biot's equations (1), and replaced by the fluid phase pressure, p :

$$v_i = \frac{\phi}{\omega^2 \tilde{\varrho}_{22}} p_{|i} - \frac{\tilde{\varrho}_{12}}{\tilde{\varrho}_{22}} u_i, \quad \left(\text{while, from one of the constitutive relations we always have } p = -\frac{\tilde{\lambda}^s v_{i|i} + \tilde{\lambda}^{\text{fs}} u_{i|i}}{\phi} \right). \quad (2)$$

The obtained equations (presented here for the case of constant material properties) are mathematically equivalent to the harmonic equations of Biot's formulation (1):

$$\begin{aligned} \overbrace{(\tilde{\lambda}^s + \mu^s)u_{j|j i} + \mu^s u_{i|j j} + \omega^2 \tilde{\varrho} u_i}^{\text{the behavior of skeleton "in vacuo"}} + \overbrace{\tilde{\gamma} p_{|i}}^{\text{a coupling term}} &= 0, \\ -\omega^2 \underbrace{\frac{\tilde{\varrho}_{22} \tilde{\gamma}}{\phi^2} u_{i|i}}_{\text{a coupling term}} + \omega^2 \underbrace{\frac{\tilde{\varrho}_{22}}{\tilde{\lambda}^f} p + p_{|i i}}_{\text{the behavior of fluid when the frame is rigid}} &= 0. \end{aligned} \quad (3)$$

In these equations the following quantities have been introduced: $\tilde{\lambda}^s \stackrel{\text{def}}{=} \tilde{\lambda}^s - \frac{(\tilde{\lambda}^{\text{fs}})^2}{\tilde{\lambda}^f}$, $\tilde{\varrho} \stackrel{\text{def}}{=} \tilde{\varrho}_{11} - \frac{(\tilde{\varrho}_{12})^2}{\tilde{\varrho}_{22}}$, and $\tilde{\gamma} \stackrel{\text{def}}{=} \phi \left(\frac{\tilde{\varrho}_{12}}{\tilde{\varrho}_{22}} - \frac{\tilde{\lambda}^{\text{fs}}}{\tilde{\lambda}^f} \right)$, whereas ϕ is the porosity. Unknowns are the solid phase displacements, u_i , and fluid phase pressure, p , so there are only 4 DOFs in every point of 3D poroelastic model.

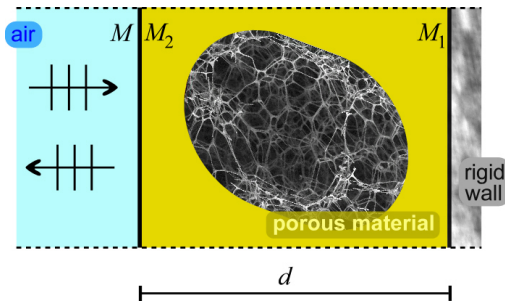
2.2 Modeling in FEMLAB[®]

FEMLAB[®] is a tool for Finite Element Analysis, especially when dealing with multiphysics problems: the user combines some FEMLAB[®] Physics modes and introduces additional coupling terms to the constitutive equations. Such an approach can be proposed when modeling piezoelectricity: the Electrostatics mode (available as one of the Electromagnetics application modes) can be combined with one of the Structural Mechanics application modes; then the multiphysics coupling needs to be added. Modeling of piezoelectricity may be even simpler since the specific Piezoelectric application modes are available from the *additional* Structural Mechanics Module (in this way the piezoelectric actuator of sandwich panel was modeled).

Unfortunately, FEMLAB[®] provides no specific module (nor mode) for porous materials. Obviously, porous materials with rigid frame are modeled using the fluid-equivalent approach, so in this case the FEMLAB[®] Fluid Dynamics mode or even the Acoustic mode can be used. Yet, there is no specific application mode or template designed for *poroelastic* materials. Moreover, the porous materials with elastic frame cannot be modeled in the multiphysics way, i.e., by using (existing) Fluid and Solid Mechanics modes to model, respectively, fluid and solid phase. This is because we have *not only* the classical multiphysics coupling (in the constitutive relations), but also a very strong coupling in the equations of equilibrium. Therefore, as a matter of fact, we have a new specific set of partial differential equations (see Equations (1) or (3)), which we need to program “from scratch” using one of the PDE modes (this is much more laborious but, obviously, the most general and flexible approach). We implemented both formulations of (harmonic) poroelasticity as 1D, 2D (plane strain state), and 3D models; we used 2nd-order Lagrange shape functions (quadratic polynomials) for all dependent variables.

2.3 Validation of poroelastic models in FEMLAB®

Tests were performed to prove the validity of the poroelastic models programmed in FEMLAB®. The tests consisted in solving the problem of propagation of harmonic waves in a layer of porous material fixed on a rigid impervious wall as presented in Figure 1. The layer oscillations were excited by the external pressure of amplitude \bar{p} (its value is of no importance since we use the linear theory, and $\bar{p} = 1$ Pa was taken in all calculations) and the angular frequency $\omega = 2\pi f$ (for different values of frequency f , see below). The final purpose was to calculate the acoustic impedance at normal incidence at the surface of the layer of porous material. For this simple 1-dimensional problem the analytical solution exists and can be found in [2]. Therefore, the comparison with the analytical results, and a mutual validation consisting in the comparison between models based on two different formulations ($u-v$ and $u-p$) could be performed.



Porous material = **glass wool** “Domisol Coffrage”:

- tortuosity, $\alpha_\infty = 1.06$,
- density of frame, $\rho_1 = 130 \text{ kg/m}^3$,
- flow resistivity, $\sigma = 40\,000 \text{ N s/m}^4$,
- porosity, $\phi = 0.94$,
- shear modulus, $\mu^s = 2.2(1 + 0.1j) \cdot 10^6 \text{ N/m}^2$,
- Poisson coefficient, $\nu = 0$,
- characteristic dimensions of the pores:
 $\Lambda = 0.56 \cdot 10^{-4} \text{ m}$, $\Lambda' = 2\Lambda = 1.12 \cdot 10^{-4} \text{ m}$.

Figure 1: A layer of porous material fixed on a rigid wall. The layer width is $d = 0.1$ m, and the material is the glass wool with characteristics presented above. An acoustic harmonic wave propagates perpendicularly onto the surface of porous material.

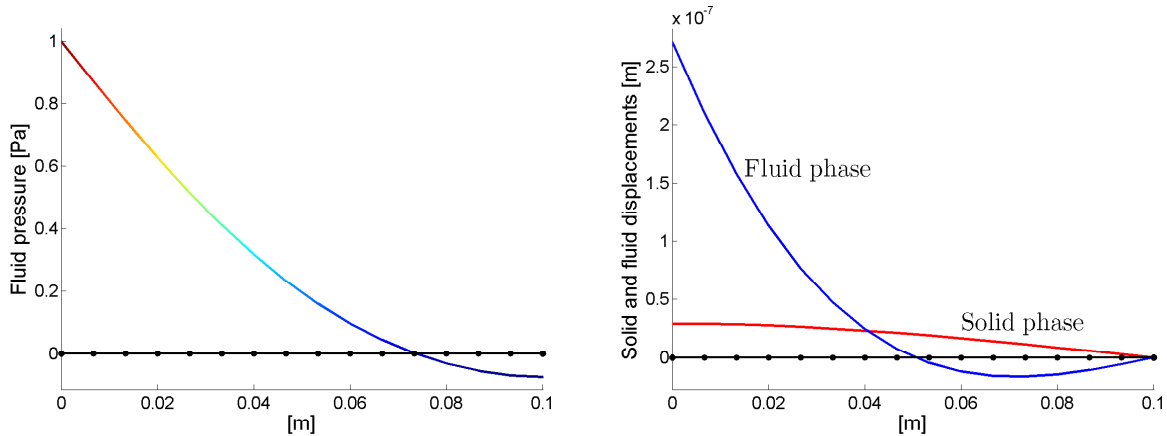


Figure 2: The mesh of 1D models and some results for the frequency $f = 300$ Hz: the fluid pressure (left), and the fluid and solid phase displacements (right).

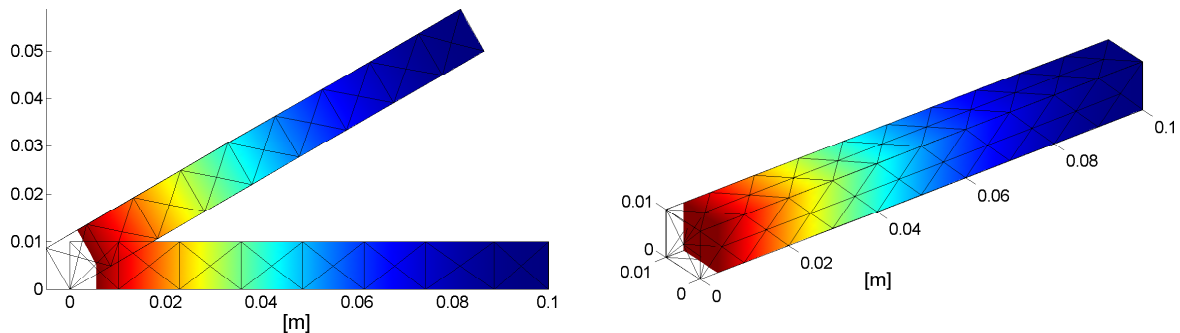


Figure 3: The meshes of 2D models (left), and 3D models (right). Scaled deformations show the solid phase and colormaps the fluid pressure obtained for the frequency $f = 300$ Hz. The colorscale can be checked in Figure 2 (left) or Figure 4 (left).

The porous material was glass wool with parameters presented in Figure 1. It was modeled in FEMLAB[®] as: 1D, 2D, and 3D poroelastic models (both formulations for every case). In the 2D and 3D cases the normal displacements on lateral boundaries were fixed to correctly model the problem. For the 2D case the problem was also modeled as *non-parallel* to the axes of the system of reference (see Figure 3 (left)) to prove the most reliable validation. The finite element meshes together with some results obtained for the frequency $f = 300$ Hz are presented in Figures 2 and 3. These and some of the following figures present the solid and fluid phase displacements as well as the fluid phase pressure. Obviously, in the case of the mixed displacement-pressure formulation, the results of FE analysis were the solid displacements and fluid pressure; the fluid displacements were calculated *a posteriori* using Equation (2)₁. Similarly, for the classical displacement formulation the FE analysis provided the solid and fluid displacements, and then the fluid pressure was calculated using Equation (2)₂. Nevertheless, we may say right now that the mutual validation turned out to be flawless: for both formulations all the models yielded “numerically identical” results of all quantities (i.e., with extremely small discrepancies – see also the comment and the end of this Section).

For every model the calculations were carried out for the frequencies from 300 Hz to 1400 Hz. The acoustic impedance was calculated using the following formula

$$Z(M) = \frac{p_{\text{air}}(M)}{\dot{v}_{\text{air}}(M)} = \frac{\bar{p}}{j\omega v_{\text{air}}(M)}, \quad \text{where } v_{\text{air}}(M) = \phi v + (1 - \phi)u \quad (4)$$

results from the condition of displacement continuity between the air and the two-phase medium. Here, $p_{\text{air}}(M)$, $\dot{v}_{\text{air}}(M)$, $v_{\text{air}}(M)$ are the pressure, velocity, and displacement of the air in point M , while u and v are the solid and fluid phase displacements parallel to the direction of propagation (i.e., perpendicular to the surface of poroelastic layer). In most cases they were equal to u_1 and v_1 , respectively. In the case of the so-called

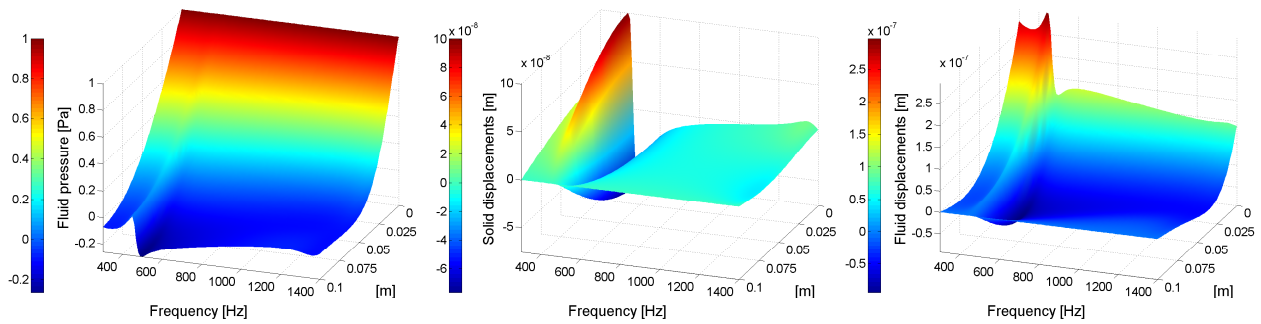


Figure 4: The fluid pressure and solid and fluid displacements in the poroelastic layer for the frequency range 300-1400 Hz. These plots were “identical” for all the numerical models.

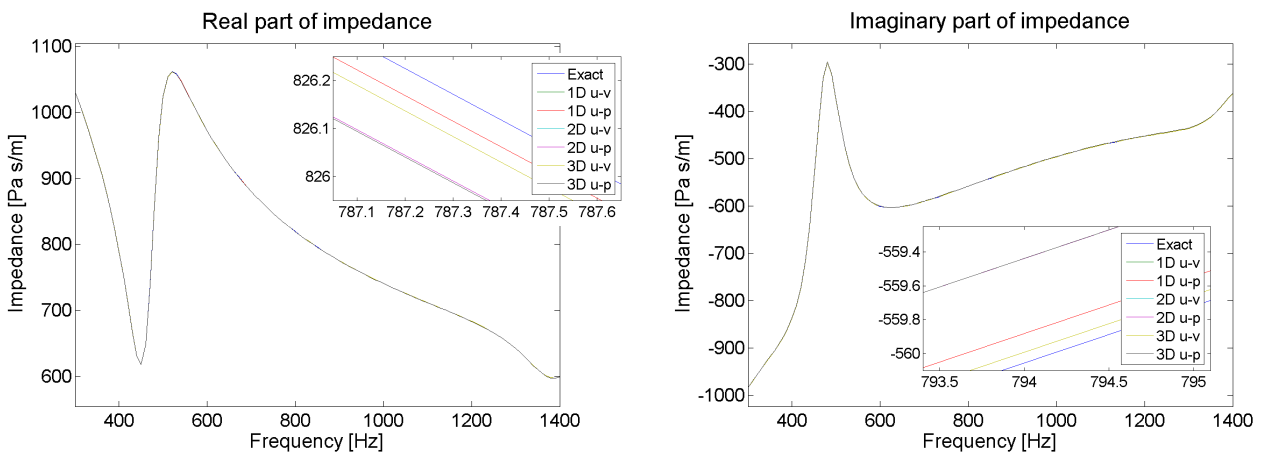


Figure 5: The acoustic impedance calculated analytically and numerically. No discrepancies can be noticed for any of the used models. The different curves can be distinguished only on the mightily zoomed plots. However, the distinction between the 1D, 2D, and 3D u - v -models cannot be even seen after zooming (all the three curves overlaid, so only the one least-recently plotted is visible). The difference between the 2D and 3D u - p -models is also extremely small.

non-parallel models they were calculated as follows: $u = u_1 \cos(\alpha) + u_2 \sin(\alpha)$, $v = v_1 \cos(\alpha) + v_2 \sin(\alpha)$, where α is the angle of the direction of propagation to the x_1 -axis. These displacements and the fluid pressure are presented in Figure 4. The “perpendicular” displacements, i.e., in the directions x_2 and x_3 , or in the case of non-parallel models calculated as $u_{\perp} = u_2 \cos(\alpha) - u_1 \sin(\alpha)$, $v_{\perp} = v_2 \cos(\alpha) - v_1 \sin(\alpha)$, were also checked and proved to be “numerically equal” zero.

Figure 5 presents the analytical and numerical calculations of the impedance. The compliance of all the numerical models with the analytical solution is extremely good. The cause for such an exquisite accuracy of numerical results lies within the fact that the problem is perfectly 1-dimensional, so the convergence of FE analysis is very fast and accurate.

3 Controlled reduction of vibroacoustic transmission: FE analysis of an active sandwich panel

3.1 Structure, geometry, and FE mesh of sandwich panel

The poroelastic models validated in the previous Section were used in modeling of sandwich panel made of two elastic faceplates and a poroelastic core. The panel is fixed alongside the lateral faces (the elastic faceplates are pin-supported). It is supposed to be an active vibrations and sound absorber so a piezoelectric actuator (composed of two piezoelectric patches) is mounted on one of the elastic layers (which therefore, we shall call by the name of *active* faceplate). The actuator was modeled using FEMLAB[®] Piezoelectricity Mode found in the additional Structural Mechanics Module. The geometry, some material data as well as the finite element mesh of the quarter of panel are presented in Figure 6. We took advantage of the symmetry of panel by applying appropriate boundary conditions.

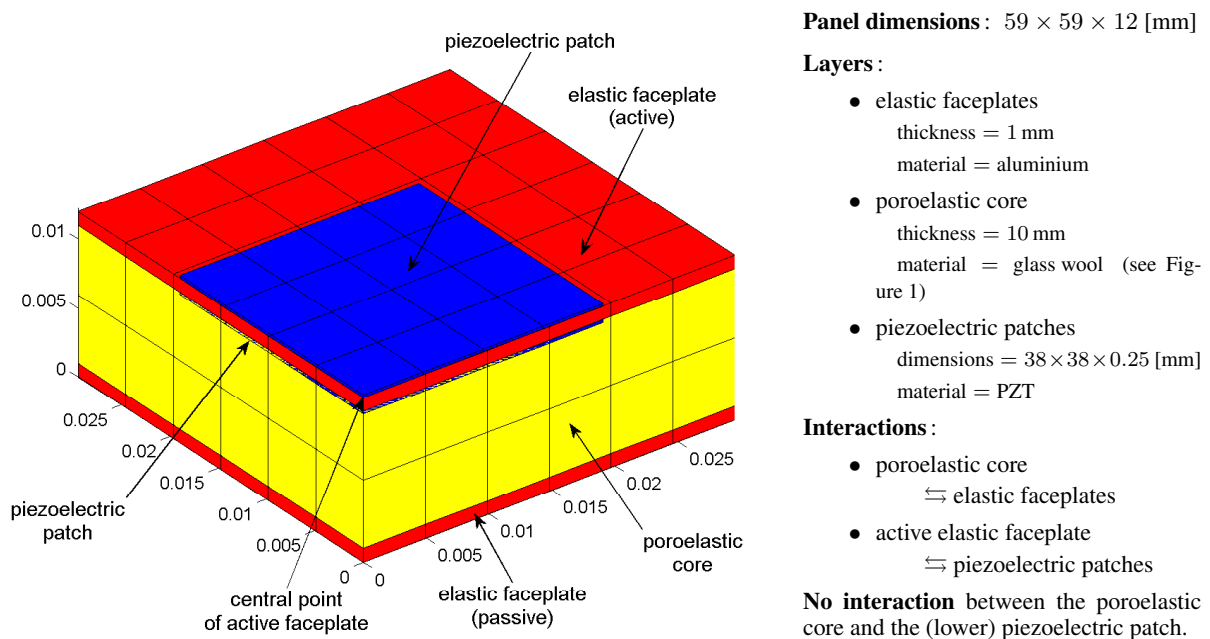


Figure 6: FE model of one quarter of sandwich panel. Panel characteristics and modeling simplifications.

3.2 Concepts of vibroacoustic control and transmission reduction analysis

The concept of vibroacoustic control using the sandwich panel can be explained as follows. An incident acoustic wave propagates onto the passive faceplate. The wave is reflected and transmitted through the panel. The piezoelectric actuator is used to excite the panel vibrations so that the normal velocity of the active faceplate is minimized which means the reduction of transmitted wave. On the active faceplate a piezoelectric sensor (not modeled here) can also be planted, so that the velocity can be measured and thus the transmission reduction process can be controlled.

In the analysis of vibroacoustic transmission reduction we shall assume that the acoustic wave is plane and harmonic. In practice, we can control transient or multi-frequency vibrations applying an appropriate signal to the actuator. This harmonic analysis, however, may also be used to control some predominant components

of vibration spectrum, and since the problem is modeled linearly, we can superpose the results obtained for different frequencies. Now, for the purpose of our analysis we define the following quantities

$$w_{p_0} \stackrel{\text{def}}{=} \frac{w_{\text{a.p.center}}^{(p_0 \neq 0, V_0=0)}}{p_0} \left[\frac{\text{m}}{\text{Pa}} \right], \quad w_{V_0} \stackrel{\text{def}}{=} \frac{w_{\text{a.p.center}}^{(p_0=0, V_0 \neq 0)}}{V_0} \left[\frac{\text{m}}{\text{V}} \right], \quad (5)$$

describing how the deflexion in the *center of active plate* depends on the excitation by acoustic pressure, p_0 , applied to the passive faceplate, or (respectively) by voltage, V_0 , applied to both piezoelectric patches fixed to the active plate. In both cases, the excitation is harmonic, and the deflections are from steady-state response for the same given frequency f ; obviously, the values p_0 and V_0 are the amplitudes of excitations.

Now, since the analysis is linear we can take advantage of the superposition principle and we can calculate the deflexion in the center of active plate for the given arbitral pressure, p_0 , and voltage, V_0 , as follows

$$w_{\text{a.p.center}} = w_{p_0} p_0 + w_{V_0} V_0. \quad (6)$$

Since the acoustic wave is plane, the biggest deflexions of the panel faceplates (under pressure excitation) are in their centers. Therefore, a low transmission means small deflection (velocity) of the center of active plate. We can control this deflexion by means of the piezoelectric actuator (and sensor). We can calculate the voltage that should be applied to the actuator by zeroing deflection in the active plate center: $w_{\text{a.p.center}} = 0$; we obtain

$$V_0 = -\frac{w_{p_0}}{w_{V_0}} p_0 = \alpha p_0, \quad \text{where we define a control coefficient } \alpha \stackrel{\text{def}}{=} -\frac{w_{p_0}}{w_{V_0}} \left[\frac{\text{V}}{\text{Pa}} \right]. \quad (7)$$

Now, for the given amplitude of acoustic pressure we should have

$$|w_{p_0, \alpha}| \stackrel{\text{def}}{=} \left| \frac{w_{\text{a.p.center}}^{(p_0 \neq 0, V_0 = \alpha p_0)}}{p_0} \right| \left[\frac{\text{m}}{\text{Pa}} \right] \approx 0 \ll |w_{p_0}|, \quad \text{and in general: } \max \left| w_{\text{whole active plate}}^{(p_0 \neq 0, V_0 = \alpha p_0)} \right| \ll |w_{p_0} p_0|,$$

which means that the vibrations of active faceplate are diminished and thus the vibroacoustic transmission is minimized. Obviously, the validity of the last inequality depends also on the form of vibrations excited by the piezoelectric actuator, and for some other panel configurations than the one presented here, may not be fully satisfied. Then, we might need to remodel the actuator, or rather take a more cumbersome criterium simultaneously minimizing the deflections in the center and some other points of active plate.

3.3 Results of FE analysis

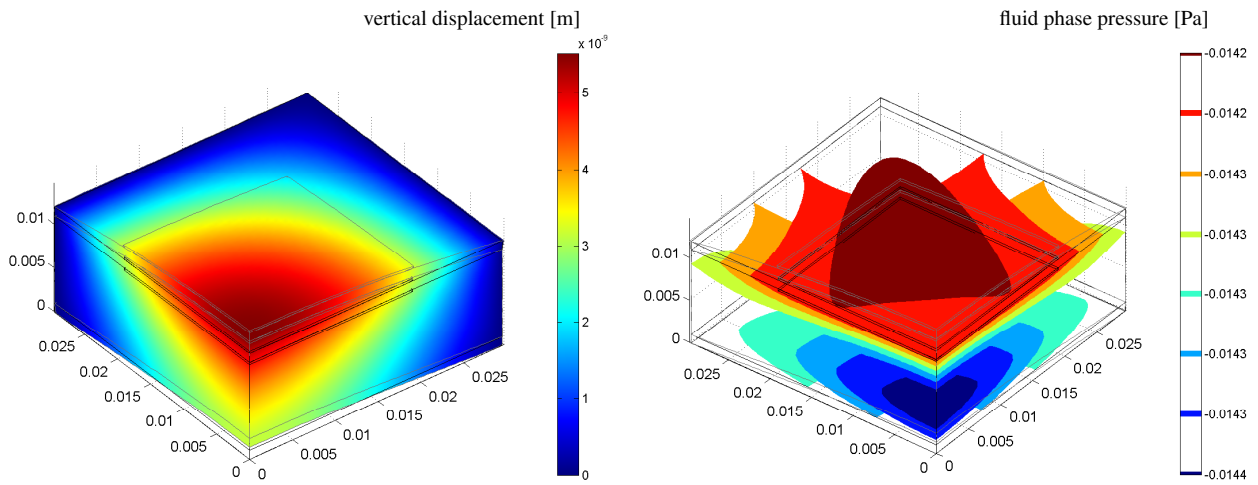
Table 1 presents some results of FE analysis of vibroacoustic transmission reduction obtained for several frequencies. Complementarily, all successive stages of analysis performed for the frequency of 400 Hz are presented in Figure 7, while Figure 8 compares only the vibrations of panel with and without control for the frequency of 1000 Hz. Finally, in Figure 9 we can compare *uncontrolled* vibroacoustic transmission through the panel excited by the harmonic acoustic waves of some higher frequencies, namely: 2, 4, and 6 kHz. Here, it is easily to notice that the amplitude of active plate displacements is strongly diminished already for the frequency of 4 kHz (though, let us repeat, no active reduction was performed: the active plate was in fact passive); in the case of 6 kHz these displacements are negligible (therefore, no active reduction is needed).

f [Hz]	w_{p_0} [$\frac{\text{m}}{\text{Pa}}$]	w_{V_0} [$\frac{\text{m}}{\text{V}}$]	α [$\frac{\text{V}}{\text{Pa}}$]	$w_{p_0, \alpha}$ [$\frac{\text{m}}{\text{Pa}}$]
200	$+5.4136 \cdot 10^{-9}$ $-4.0743 \cdot 10^{-10} \cdot j$	$-3.9269 \cdot 10^{-8}$ $+2.4664 \cdot 10^{-8} \cdot j$	$+1.0353 \cdot 10^{-1}$ $+5.4651 \cdot 10^{-2} \cdot j$	$-1.1959 \cdot 10^{-18}$ $-1.4975 \cdot 10^{-19} \cdot j$
400	$+5.4928 \cdot 10^{-9}$ $-3.8361 \cdot 10^{-10} \cdot j$	$-3.4592 \cdot 10^{-8}$ $+2.3640 \cdot 10^{-8} \cdot j$	$+1.1341 \cdot 10^{-1}$ $+6.6412 \cdot 10^{-2} \cdot j$	$+2.7335 \cdot 10^{-18}$ $-7.8865 \cdot 10^{-19} \cdot j$
700	$+5.7625 \cdot 10^{-9}$ $-3.1800 \cdot 10^{-10} \cdot j$	$-2.1294 \cdot 10^{-8}$ $+2.1212 \cdot 10^{-8} \cdot j$	$+1.4330 \cdot 10^{-1}$ $+1.2781 \cdot 10^{-1} \cdot j$	$-1.8934 \cdot 10^{-18}$ $+2.0090 \cdot 10^{-19} \cdot j$
1000	$+6.3667 \cdot 10^{-9}$ $-2.0573 \cdot 10^{-10} \cdot j$	$+1.5265 \cdot 10^{-9}$ $+1.8487 \cdot 10^{-8} \cdot j$	$-1.7190 \cdot 10^{-2}$ $+3.4296 \cdot 10^{-1} \cdot j$	$-7.3485 \cdot 10^{-19}$ $+1.5381 \cdot 10^{-18} \cdot j$
1500	$+9.9421 \cdot 10^{-9}$ $+4.2990 \cdot 10^{-10} \cdot j$	$+9.3573 \cdot 10^{-8}$ $+2.0541 \cdot 10^{-8} \cdot j$	$-1.0233 \cdot 10^{-1}$ $+1.7868 \cdot 10^{-2} \cdot j$	$+2.6626 \cdot 10^{-18}$ $+3.0025 \cdot 10^{-19} \cdot j$
2000	$-3.4683 \cdot 10^{-8}$ $+3.0667 \cdot 10^{-8} \cdot j$	$-7.4316 \cdot 10^{-7}$ $+6.4889 \cdot 10^{-7} \cdot j$	$-4.6925 \cdot 10^{-2}$ $+2.9242 \cdot 10^{-4} \cdot j$	$+7.2414 \cdot 10^{-17}$ $-2.4210 \cdot 10^{-17} \cdot j$
4000	$-6.1747 \cdot 10^{-10}$ $+2.0959 \cdot 10^{-11} \cdot j$	$-4.3402 \cdot 10^{-8}$ $+4.7801 \cdot 10^{-9} \cdot j$	$-1.4109 \cdot 10^{-2}$ $-1.0710 \cdot 10^{-3} \cdot j$	$+9.8038 \cdot 10^{-21}$ $-2.5750 \cdot 10^{-20} \cdot j$

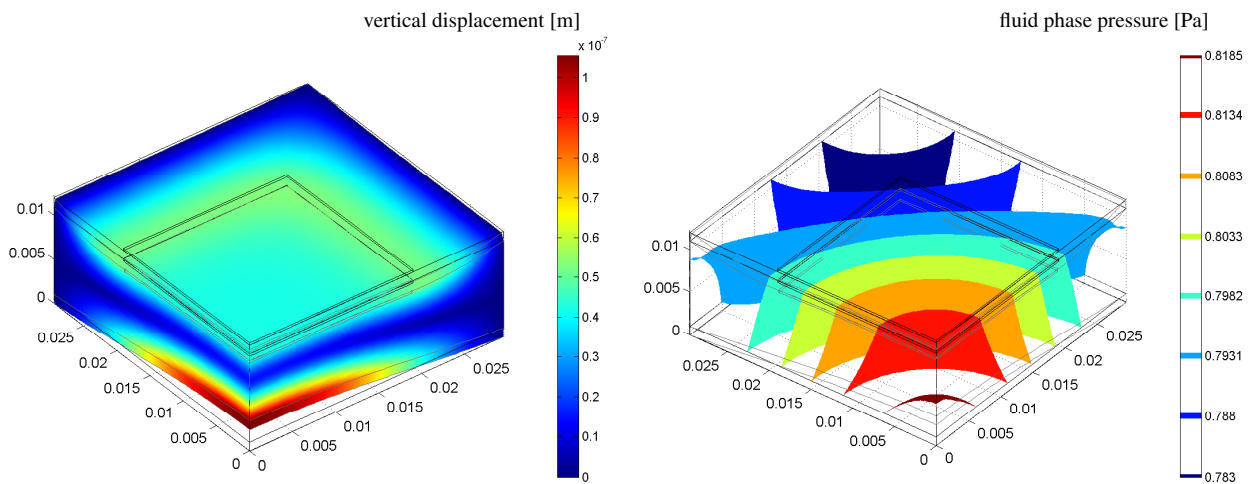
Table 1: Results of FE analysis of vibroacoustic transmission reduction.

Excitation frequency: $f = 400$ Hz

- excitation with the **acoustic pressure**, $p_0 = 1$ Pa, without control ($V_0 = 0$ V)



- excitation with the **piezo-device**, $V_0 = 1$ V, without acoustic pressure ($p_0 = 0$ Pa)



- excitation with the **acoustic pressure**, $p_0 = 1$ Pa, **with the piezo-device control**, $V_0 = \alpha p_0$

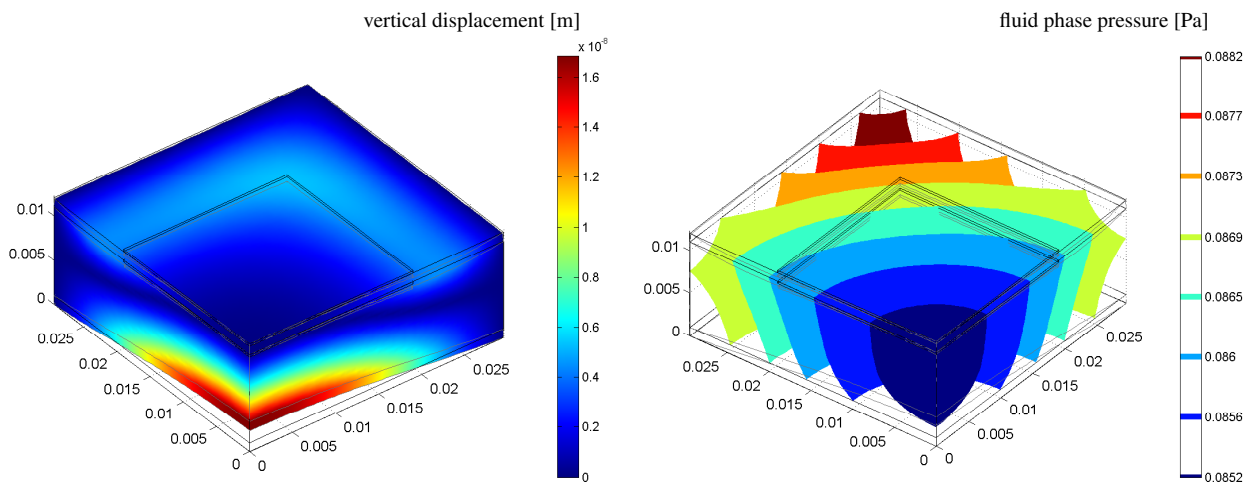


Figure 7: Panel deformation, its vertical displacements, and pressure in the fluid phase of poroelastic core. Harmonic vibrations with frequency 400 Hz.

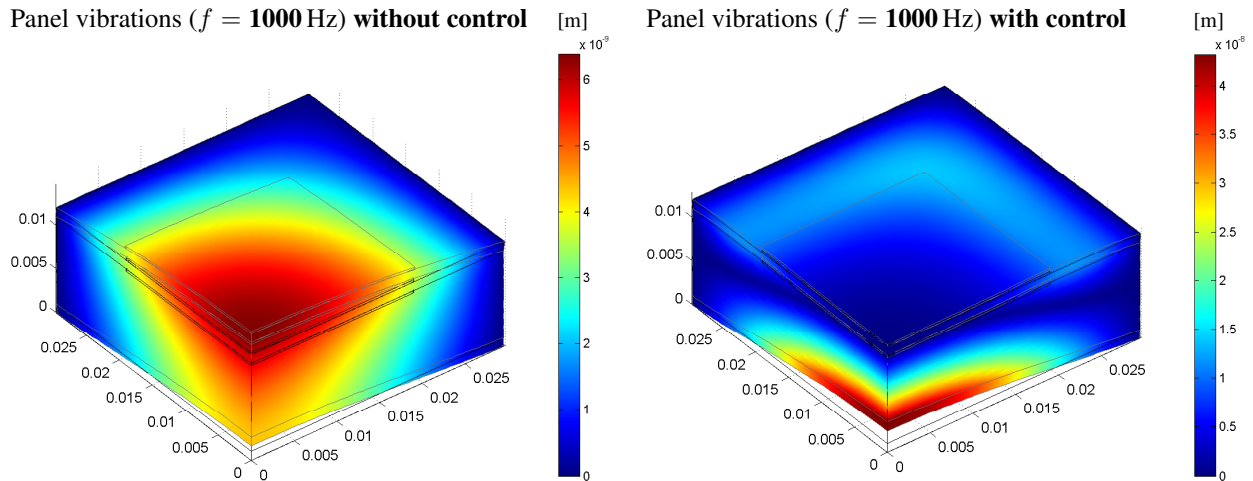


Figure 8: Panel vibrations **with** and **without control** for harmonic frequency of 1000 Hz.

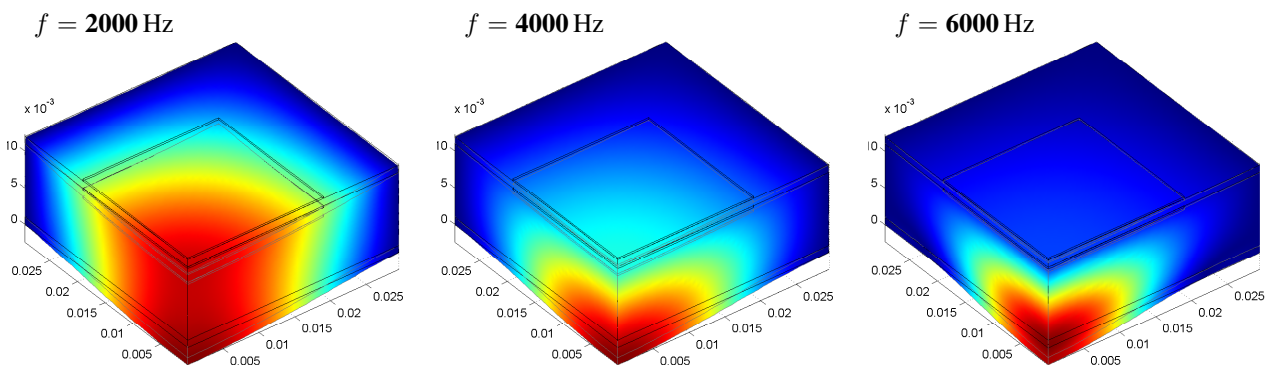


Figure 9: Panel vibrations **without control** for harmonic frequencies: 2, 4, and 6 kHz.

4 Final remarks and perspectives

The results presented above prove that the proposed prototype of sandwich panel should work properly for a wide frequency range as an efficient active/passive reducer of vibroacoustic transmission. They also illustrate the vital fact that for high frequencies the vibroacoustic transmission is reduced passively (see Figure 9). We should also remind that for higher frequencies the most of porous media behave like materials with rigid frame (i.e., the elastic vibrations of skeleton tend to be negligible), so that much simpler (fluid-equivalent) models can be used. However, for vibroacoustic applications in the low frequency range (where the active reduction proves its necessity) the presented-here poroelastic modeling *must* be applied.

The model of sandwich panel was implemented in FEMLAB[®], and so it can be easily used in MATLAB[®] environment. This modeling allows us *not only* a reliable validation of passive or active elasto-poroelastic panels, or prediction of vibroacoustic transmission loss, but – first of all – enables us to efficiently perform any parametric survey and configuration optimization of these panels to determine the best assembly and the best control strategy for reducing the vibroacoustic transmission over a wide frequency range.

References

- [1] M. A. Biot, *The theory of propagation of elastic waves in a fluid-saturated porous solid*, J. Acoust. Soc. Am. **28**, pp. 168-191, 1956.
- [2] J. F. Allard, *Propagation of Sound in Porous Media. Modelling Sound Absorbing Materials*, Elsevier, 1993.
- [3] N. Atalla, R. Panneton, and P. Debergue, *A mixed displacement-pressure formulation for poroelastic materials*, J. Acoust. Soc. Am. **104**, pp. 1444-1452, 1998.
- [4] P. Debergue R. Panneton, and N. Atalla, *Boundary conditions for the weak formulation of the mixed (u, p) poroelasticity problem*, J. Acoust. Soc. Am. **106**, pp. 2383-2390, 1999.